The Fermi Gamma-Ray Space Telescope Discovers the Pulsar in the Young Galactic Supernova Remnant CTA 1

A. A. Abdo,[1,2] M. Ackermann,[3] W. B. Atwood,[4] L. Baldini,[5] J. Ballet,[6] G. Barbiellini,[7,8] M. G. Baring,[9] D. Bastieri,[10,11] B. M. Baughman,[12] K. Bechtol,[3] R. Bellazzini,[5] B. Berenji,[3] R. D. Blandford,[3] E. D. Bloom,[3] G. Bogaert,[13] E. Bonamente,[14,15] A. W. Borgland,[3] J. Bregeon,[5] A. Brez,[5] M. Brigida,[16,17] P. Bruel,[13] T. H. Burnett,[18] G. A. Caliandro,[16,17] R. A. Cameron,[3] P. A. Caraveo,[19] P. Carlson,[20] J. M. Casandjian,[6] C. Cecchi,[14,15] E. Charles,[3] A. Chekhtman,[2,21] C. C. Cheung,[22] J. Chiang,[3] S. Ciprini,[14,15] R. Claus,[3] J. Cohen-Tanugi,[23] L. R. Cominsky,[24] J. Conrad,[20,25] S. Cutini,[26] D. S. Davis,[2,27] C. D. Dermer,[2] A. de Angelis,[28] F. de Palma,[16,17] S. W. Digel,[3] M. Dormody,[4] E. do Couto e Silva,[3] P. S. Drell,[3] R. Dubois,[3] D. Dumora,[29,30] Y. Edmonds,[3] C. Farnier,[23] W. B. Focke,[3] Y. Fukazawa,[31] S. Funk,[3] P. Fusco,[16,17] F. Gargano,[17] D. Gasparrini,[26] N. Gehrels,[22,32] S. Germani,[14,15] B. Giebels,[13] N. Giglietto,[16,17] F. Giordano,[16,17] T. Glanzman,[3] G. Godfrey,[3] I. A. Grenier,[6] M.-H. Grondin,[29,30] J. E. Grove,[2] L. Guillemot,[29,30] S. Guiriec,[23] A. K. Harding,[22] R. C. Hartman,[22] E. Hays,[22] R. E. Hughes,[12] G. Jóhannesson,[3] A. S. Johnson,[3] R. P. Johnson,[4] T. J. Johnson,[22,32] W. N. Johnson,[2] T. Kamae,[3] Y. Kanai,[33] G. Kanbach,[34]* H. Katagiri,[31] N. Kawai,[33, 35] M. Kerr,[18] T. Kishishita,[36] B. Kiziltan,[37] J. Knödlseder,[38] M. L. Kocian,[3] N. Komin,[6,23]† F. Kuehn,[12] M. Kuss,[5] L. Latronico,[5] M. Lemoine-Goumard,[29,30] F. Longo,[7,8] V. Lonjou,[29,30] F. Loparco,[16,17] B. Lott,[29,30] M. N. Lovellette,[2] P. Lubrano,[14,15] A. Makeev,[21] M. Marelli,[19] M. N. Mazziotta,[17] J. E. McEnery,[22] S. McGlynn,[20] C. Meurer,[25] P. F. Michelson,[3] T. Mineo,[39] W. Mitthumsiri,[3] T. Mizuno,[31] A. A. Moiseev,[40] C. Monte,[16,17] M. E. Monzani,[3] A. Morselli,[41] I. V. Moskalenko,[3] S. Murgia,[3] T. Nakamori,[33] P. L. Nolan,[3] E. Nuss,[23] M. Ohno,[36] T. Ohsugi,[31] A. Okumura,[42] N. Omodei,[5] E. Orlando,[34] J. F. Ormes,[43] M. Ozaki,[36] D. Paneque,[3] J. H. Panetta,[3] D. Parent,[29,30] V. Pelassa,[23] M. Pepe,[14,15] M. Pesce-Rollins,[5] G. Piano,[41] L. Pieri,[10] F. Piron,[23] T. A. Porter,[4] S. Rainò,[16,17] R. Rando,[10,11] P. S. Ray,[2] M. Razzano,[5] A. Reimer,[3] O. Reimer,[3] T. Reposeur,[29,30] S. Ritz,[22,32] L. S. Rochester,[3] A. Y. Rodriguez,[44] R. W. Romani,[3] M. Roth,[18] F. Ryde,[20] H. F.-W. Sadrozinski,[4] D. Sanchez,[13] A. Sander,[12] P. M. Saz Parkinson,[4] T. L. Schalk,[4] A. Sellerholm,[25] C. Sgrò,[5] E. J. Siskind,[45] D. A. Smith,[29,30] P. D. Smith,[12] G. Spandre,[5] P. Spinelli,[16,17] J.-L. Starck,[6] M. S. Strickman,[2] D. J. Suson,[46] H. Tajima,[3] H. Takahashi,[31] T. Takahashi,[36] T. Tanaka,[3] J. B. Thayer,[3] J. G. Thayer,[3] D. J. Thompson,[22] S. E. Thorsett,[4] L. Tibaldo,[10,11] D. F. Torres,[44,47] G. Tosti,[14,15] A. Tramacere,[3,48] T. L. Usher,[3] A. Van Etten,[3] N. Vilchez,[38] V. Vitale,[41] P. Wang,[3] K. Watters,[3] B. L. Winer,[12] K. S. Wood,[2]* H. Yasuda,[31] T. Ylinen,[20,49] M. Ziegler[4]*

Energetic young pulsars and expanding blast waves [supernova remnants (SNRs)] are the most visible remains after massive stars, ending their lives, explode in core-collapse supernovae. The Fermi Gamma-Ray Space Telescope has unveiled a radio quiet pulsar located near the center of the compact synchrotron nebula inside the supernova remnant CTA 1. The pulsar, discovered through its gamma-ray pulsations, has a period of 316.86 milliseconds and a period derivative of 3.614×10^{-13} seconds per second. Its characteristic age of 10^4 years is comparable to that estimated for the SNR. We speculate that most unidentified Galactic gamma-ray sources associated with star-forming regions and SNRs are such young pulsars.

After the discovery of radio pulsars in the late 1960s, some clear supernova remnant (SNR)–pulsar associations were discovered (most notably the Crab and Vela systems). Observations in the radio, x-ray, and gamma-ray bands with increasing sensitivity during the past 30 years have added many more SNR/pulsar associations. Yet we are still far from the complete census of these products of massive star deaths, which is needed to study a major population of stellar and Galactic astronomy. Here we report the discovery of a gamma-ray pulsar with a spin period of 316 ms, coinciding with the previously known gamma-ray source 3EG J0010+7309, thus confirming the identification of the neutron star (NS) powering the pulsar wind nebula (PWN) and the gamma-ray source. This pulsar detection implies that many of the yet-unidentified low-latitude Galactic gamma-ray sources also could be pulsars.

A survey of radio sources conducted at 960 MHz with the Owens Valley Radio Observatory in the 1960s led to the discovery of a previously uncataloged extended source (*1*), designated CTA 1, as the first object in Caltech's catalog A. Follow-up radio surveys (*2*–*7*) with increased sensitivity and angular resolution showed that CTA 1 has the typical morphology of a shell-type SNR with an incomplete shell of filaments and extended emission from a broken shell roughly circular and ~90 arc min in diameter (Fig. 1). The excitation of atomic lines in the shocked interstellar medium with well-defined optical filaments (*8*) lends further support to the identification of CTA 1 as a young SNR in the Sedov phase of expansion. The radio and x-ray characteristics of CTA 1 imply that it is 1.4 ± 0.3 kpc away (*6*) and that it exploded 5000 to 15,000 years ago (*6*, *9*, *10*).

Imaging and spectroscopy of CTA 1 with *ROSAT* (*11*), *ASCA* (*9*), *XMM* (*10*), and Chandra (*12*) revealed a typical center-filled or composite SNR with a central point source, RXJ0007.0+7303, embedded in a compact nebula, and a jetlike extension (*12*). The offset of the x-ray source from the geometrical center of the SNR suggested that it has a transverse velocity (*11*) of ~450 km s^{-1}. The natural interpretation of these data are that of a young NS, visible both in thermal surface and nonthermal magnetospheric emission (*12*), powering a synchrotron PWN. The thermal spectrum from the NS (*11*, *12*) is not easily interpreted: The temperature is too high and the required emission area is too small if the NS has no atmosphere. A particle-heated polar cap could be a possibility. Alternatively, if the NS has a light element atmosphere and cools through a direct Urca process, a cooling age of (1 to 2) $\times 10^4$ years is also possible (*11*). Although no signs of periodicity could be found in the x-ray data (*11*), the energetics of the PWN lead to typical requirements for the time-averaged spin-down power of the putative pulsar of 10^{36} to 10^{37} erg s^{-1}. Very deep searches (*12*) for a counterpart of the x-ray source in radio and optical wavebands resulted only in upper limits. If RX J0007.0+7303 is indeed a radio pulsar, its radio luminosity is an order of magnitude below the faintest radio pulsars known (*12*). It is likely that the radio beam does not intersect the Earth.

High-energy emission (>100 MeV) from the *EGRET* source 3EG J0010+7309 matches RX J0007.0+7303 spatially, although the *EGRET* position uncertainty is very large (*13*). The position derived from *EGRET* photons above 1 GeV (*14*) at galactic longitude l and latitude b = 119.87, 10.52 with an error radius of 11 arc min (95% confidence) overlaps even better with the ROSAT source (l, b = 119.6602, 10.4629). It has thus been suggested that the 3EG source is an unresolved source in CTA 1 (*14*), or, more generally, that several unidentified gamma-ray sources are associated with SNRs (*15*). However, confirmation of such SNR associations based on imaging was not possible with the *EGRET* angular resolution. The CTA 1 gamma-ray source shows all indications of being a young pulsar: The gamma-ray flux was constant through the epochs of *EGRET* observations (1991 to 1995), and the spectrum showed a hard power law with an index of -1.6 ± 0.2 and a spectral steepening above ~2 GeV (*14*), which is similar to other *EGRET* pulsars like Geminga and Vela. For an assumed pulsar beam of 1 sr (and taking into account the uncertainty in distance), the observed gamma-ray flux corresponds to a luminosity of $(4 \pm 2) \times 10^{33}$ erg s^{-1}, which is well within the range of the luminosities of Geminga [9×10^{32} erg s^{-1}, $P \sim 237$ ms (where P is the spin period)] and Crab (4×10^{34} erg s^{-1}, $P \sim 33$ ms).

On 11 June 2008, the Fermi Gamma-Ray Space Telescope was launched into a low Earth

orbit (*16*). The imaging gamma-ray telescope LAT (Large Area Telescope), Fermi's main instrument, covers the energy range from 20 MeV up to >300 GeV with a sensitivity that exceeds that of *EGRET*. The first exposures of the region of CTA 1 were made during the commissioning phase of Fermi LAT (30 June to 30 July 2008) and in the initial days (5 to 20 August 2008) of routine operations. Although the telescope was not yet fully tuned and calibrated during commissioning, >900 gamma-ray photons above 100 MeV from 3EG J0010+7309 were recorded during these exposures [see supporting online material (SOM)], which amounts to ~2.6 times the number collected with *EGRET* from this source over its entire mission.

A bright gamma-ray source is detected at l,b = 119°.652, 10°.468 with a 95% (statistical) error circle radius of 0°.038 (a systematic error of ~0°.02 is not included). Figure 1 shows the LAT source and the x-ray source RX J00070+7302, which is located central to the PWN, superimposed on the radio map at 1420 MHz (*7*). These fall on the edge of 3EG J0010+7309 (l,b = 119.92, 10.54) and its 95% error circle of radius 0.24°. The measured flux of the LAT source is $(3.8 \pm 0.2) \times 10^{-7}$ photons (>100 MeV) cm^{-2} s^{-1}, with an additional systematic uncertainty of 30%, owing to the ongoing calibration of the instrument, which is consistent with the *EGRET* measured flux of $(4.2 \pm 0.5) \times 10^{-7}$ ph cm^{-2} s^{-1} (*13*).

The arrival times of the LAT photons, which are recorded with 300-ns accuracy and referenced to the Fermi satellite Global Positioning System clock, were corrected to the solar system barycenter (SSB) using the JPL DE405 solar system ephemeris and the Chandra x-ray position (Table 1). Photons with energy >100 MeV were selected within a radius of 1° around the source position and searched for periodicity. The results described here are not altered substantially if photons within selection radii between 0.7° and 2.5° are used.

Application of a new search technique based on photon arrival-time differencing (*17*)—which is highly efficient for sparse photon data—and refining and fitting the detections with the pulsar analysis packages PRESTO (*18*) and Tempo2 (*19*) resulted in the detection of strong pulsations in the selected photons (see SOM). Figure S1 shows that the pulsations are markedly present over the complete time interval of observation. The pulsar rotational ephemeris is given in Table 1.

By extracting photons around the Vela pulsar from the same set of observations and applying the same analysis procedures, we found the rotational ephemeris for the Vela pulsar to be in good agreement with the values obtained by the LAT radio pulsar timing collaboration (*20*).

A contour plot of period-period derivative search space reveals the pulsar (Fig. 2), as does the resulting gamma-ray light curve above 100 MeV (Fig. 3).

A NS with a moment of inertia of $I = 1.0 \times 10^{45}$ g cm^2 and angular frequency ω is assumed to lose its rotational energy through magnetic dipole radiation and follow a braking law of $\dot{\omega}\alpha - \omega^3$. This can be integrated to yield the characteristic age $\tau = \omega/2\dot{\omega}$, which is a coarse estimate of the true age of a pulsar. The spin-down power $\dot{E}_{\rm rot} = I\omega\dot{\omega}$ and the dipole magnetic field strength, $B = 3.2 \times 10^{19}\sqrt{P\dot{P}}$ G, also follow from the parameters of rotation.

For the CTA 1 pulsar, we derive a characteristic age of ~1.4×10^4 years, a spin-down power of ~4.5×10^{35} erg s^{-1}, and a surface magnetic field strength of 1.1×10^{13} G. This field strength is higher than any of the *EGRET* detected pulsars and second highest among known gamma-ray pulsars. PSR J1509-58, with an inferred field of 1.54×10^{13} G, shows emission only up to ~30 MeV, whereas emission from the CTA 1 pulsar is present to at least 5 GeV.

We searched archival data of exposures by *XMM*, *ASCA*, Chandra, and *EGRET* for periods near that extrapolated from the LAT ephemeris. The pulsar was not strongly detected in these data (*21*).

[1]National Research Council Research Associate, National Academy of Sciences, Washington, DC 20001, USA. [2]Space Science Division, Naval Research Laboratory, Washington, DC 20375, USA. [3]W. W. Hansen Experimental Physics Laboratory, Kavli Institute for Particle Astrophysics and Cosmology, Department of Physics and Stanford Linear Accelerator Center, Stanford University, Stanford, CA 94305, USA. [4]Santa Cruz Institute for Particle Physics, Department of Physics and Department of Astronomy and Astrophysics, University of California at Santa Cruz, Santa Cruz, CA 95064, USA. [5]Istituto Nazionale di Fisica Nucleare, Sezione di Pisa, I-56127 Pisa, Italy. [6]Laboratoire Astrophysique, Interactions, Multi-échelles–Commissariat à l'Énergie Atomique (CEA)–CNRS-Université Paris Diderot, Service d'Astrophysique, CEA Saclay, F-91191 Gif sur Yvette, France. [7]Istituto Nazionale di Fisica Nucleare, Sezione di Trieste, I-34127 Trieste, Italy. [8]Dipartimento di Fisica, Università di Trieste, I-34127 Trieste, Italy. [9]Rice University, Department of Physics and Astronomy, MS-108, Post Office Box 1892, Houston, TX 77251, USA. [10]Istituto Nazionale di Fisica Nucleare, Sezione di Padova, I-35131 Padova, Italy. [11]Dipartimento di Fisica "G. Galilei," Università di Padova, I-35131 Padova, Italy. [12]Department of Physics, Center for Cosmology and Astro-Particle Physics, The Ohio State University, Columbus, OH 43210, USA. [13]Laboratoire Leprince-Ringuet, École Polytechnique, CNRS/IN2P3, Palaiseau, France. [14]Istituto Nazionale di Fisica Nucleare, Sezione di Perugia, I-06123 Perugia, Italy. [15]Dipartimento di Fisica, Università degli Studi di Perugia, I-06123 Perugia, Italy. [16]Dipartimento di Fisica "M. Merlin" dell'Università e del Politecnico di Bari, I-70126 Bari, Italy. [17]Istituto Nazionale di Fisica Nucleare, Sezione di Bari, 70126 Bari, Italy. [18]Department of Physics, University of Washington, Seattle, WA 98195–1560, USA. [19]Istituto Nazionale di Astrofisica–Istituto di Astrofisica Spaziale e Fisica Cosmica, I-20133 Milano, Italy. [20]Department of Physics, Royal Institute of Technology (Kungliga Tekniska Högskolan), AlbaNova, SE-106 91 Stockholm, Sweden. [21]George Mason University, Fairfax, VA 22030, USA. [22]NASA Goddard Space Flight Center, Greenbelt, MD 20771, USA. [23]Laboratoire de Physique Théorique et Astroparticules, Université Montpellier 2, CNRS/IN2P3, Montpellier, France. [24]Department of Physics and Astronomy, Sonoma State University, Rohnert Park, CA 94928–3609, USA. [25]Department of Physics, Stockholm University, AlbaNova, SE-106 91 Stockholm, Sweden. [26]Agenzia Spaziale Italiana Science Data Center, I-00044 Frascati (Roma), Italy. [27]Center for Space Sciences and Technology, University of Maryland, Baltimore County, Baltimore, MD 21250, USA. [28]Dipartimento di Fisica, Università di Udine and Istituto Nazionale di Fisica Nucleare, Sezione di Trieste, Gruppo Collegato di Udine, I-33100 Udine, Italy. [29]CNRS/IN2P3, Centre d'Études Nucléaires Bordeaux Gradignan, UMR 5797, Gradignan, 33175, France. [30]Université de Bordeaux, Centre d'Études Nucléaires Bordeaux Gradignan, UMR 5797, Gradignan, 33175, France. [31]Department of Physical Science and Hiroshima Astrophysical Science Center, Hiroshima University, Higashi-Hiroshima 739-8526, Japan. [32]University of Maryland, College Park, MD 20742, USA. [33]Department of Physics, Tokyo Institute of Technology, Meguro-ku, Tokyo 152-8551, Japan. [34]Max-Planck-Institut für Extraterrestrische Physik, Giessenbachstraße, 85748 Garching, Germany. [35]Cosmic Radiation Laboratory, Institute of Physical and Chemical Research (RIKEN), Wako, Saitama 351-0198, Japan. [36]Institute of Space and Astronautical Science, Japan Aerospace Exploration Agency (JAXA), 3-1-1 Yoshinodai, Sagamihara, Kanagawa 229-8510, Japan. [37]University of California Observatories/Lick Observatories, 1156 High Street, Santa Cruz, CA 95064, USA. [38]Centre d'Étude Spatiale des Rayonnements, CNRS/UPS, BP 44346, F-30128 Toulouse Cedex 4, France. [39]Istituto di Astrofisica Spaziale e Fisica Cosmica Palermo, 90146 Palermo, Italy. [40]Center for Research and Exploration in Space Science and Technology, NASA Goddard Space Flight Center, Greenbelt, MD 20771, USA. [41]Istituto Nazionale di Fisica Nucleare, Sezione di Roma "Tor Vergata" and Dipartimento di Fisica, Università di Roma "Tor Vergata," I-00133 Roma, Italy. [42]Department of Physics, Graduate School of Science, University of Tokyo, 7-3-1 Hongo, Bunkyo-ku, Tokyo 113-0033, Japan. [43]Department of Physics and Astronomy, University of Denver, Denver, CO 80208, USA. [44]Institut de Ciencies de l'Espai (Institut d'Estudis Espacials de Catalunya–Consejo Superior de Investigaciones Científicas), Campus Universitat Autonoma de Barcelona, 08193 Barcelona, Spain. [45]NYCB Real-Time Computing Inc., 18 Meudon Drive, Lattingtown, NY 11560–1025, USA. [46]Department of Chemistry and Physics, Purdue University Calumet, Hammond, IN 46323–2094, USA. [47]Institució Catalana de Recerca i Estudis Avançats, Barcelona, Spain. [48]Consorzio Interuniversitario per la Fisica Spaziale, I-10133 Torino, Italy. [49]School of Pure and Applied Natural Sciences, University of Kalmar, SE-391 82 Kalmar, Sweden.

*To whom correspondence should be addressed. E-mail: gok@mpe.mpg.de (G.K.); kent.wood@nrl.navy.mil (K.S.W.); ziegler@scipp.ucsc.edu (M.Z.)

†Present address: Laboratoire Astrophysique, Interactions, Multi-échelles–Commissariat à l'Energie Atomique (CEA)–CNRS-Université Paris Diderot, Service d'Astrophysique, CEA Saclay, F-91191 Gif sur Yvette, France.

Table 1. Rotational ephemeris for the pulsar in CTA 1. The numbers in parentheses indicate the error in the last decimal digit. For the SSB correction, the position of the Chandra x-ray source (*12*) was assumed.

Frequency (Hz)	Frequency derivative (s^{-2})	Period (ms)	Period derivative (s s^{-1})	Epoch [MJD (TDB)]	R.A. (J2000.0)	DEC. (J2000.0)	Galactic longitude	Galactic latitude
3.165922467(9)	−3.623(4) × 10^{-12}	315.8637050(9)	3.615(4) × 10^{-13}	54647.440 938	00^h 07^m $01^s.56$	+73° 03′ 08″.1	119°.65947(3)	+10°.463348(3)

The new pulsar in CTA 1 exhibits all of the characteristics of a young high-energy pulsar, which powers a synchrotron PWN embedded in a larger SNR. The spin-down power of the CTA 1 pulsar of ~4.5×10^{35} erg s^{-1} is sufficient to supply the PWN with magnetic fields and energetic electrons at the required rate of 10^{35} to 10^{36} erg s^{-1} (*10*), and the pulsar age is consistent with the inferred age for the SNR. With its spin-down power of ~4.5×10^{38} erg s^{-1}, the Crab pulsar supplies the Crab nebula with its requirement of ~10^{38} erg s^{-1} with a similar efficiency (*22*). Comparing the total luminosity from the CTA 1 pulsar inferred from the LAT flux measured for 3EG J0010+7309 to the pulsar spin-down power, we estimate an efficiency of converting spin-down power into pulsed gamma rays that is ~1%, if the emission is beamed into a solid angle of 1 sr. The Vela pulsar, which is of similar age, has a gamma-ray efficiency of 0.1%; however, PSR B1706-44 (*23*) (with an age of 1.7×10^4 years) has an efficiency of 1.9%, and the much older Geminga pulsar (3.4×10^5 years) converts its spin-down into energetic gamma-rays with an efficiency of ~3%.

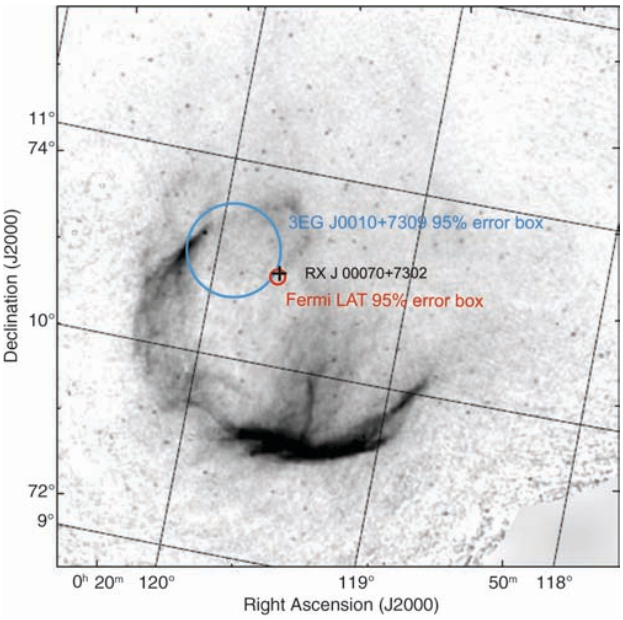

Fig. 1. The Fermi LAT gamma-ray source, central PWN x-ray source, and corresponding *EGRET* source superimposed on a 1420-MHz map (*7*) of CTA 1. The LAT source and its 95% error region (small red circle) is displayed on the map, together with the central PWN source RX J00070+7302 (black cross) and the position and error of the corresponding *EGRET* source 3EG J0010+7309 (large blue circle). The coincidence of the pulsed gamma-ray source and the x-ray point source embedded in the off-center PWN is notable. The offset of the pulsar from the center of the radio SNR, which is thought to be the place of origin, is quite visible. The inferred transverse speed of the pulsar is ~450 km s^{-1}, which is a reasonable speed of a pulsar (*30*).

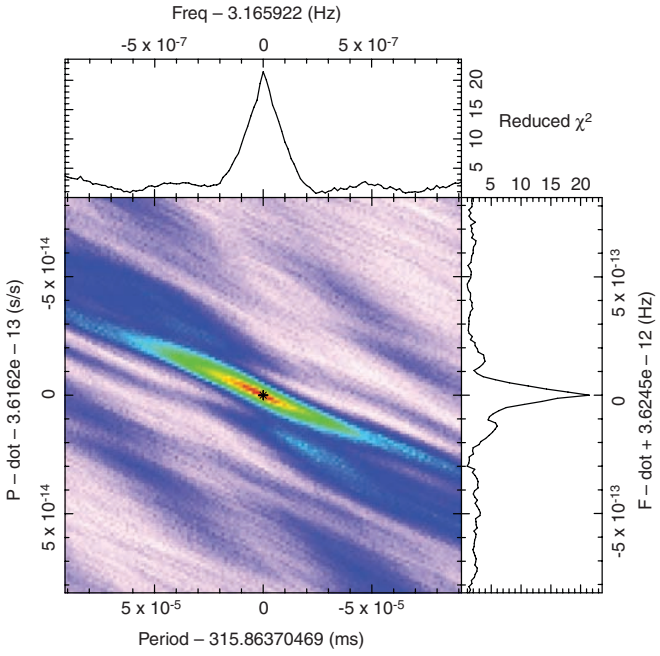

Fig. 2. Contours of detection significance over a range of period and period derivative using photons within a radius of 1° around RXJ0007.0+7303. The initial indication of a signal in this $P, \dot{P}$ region was found with a search technique that uses photon arrival-time differencing (*17*), whereas the determination of the exact ephemeris makes use of the tools PRESTO and Tempo2 (*18*, *19*).

The gamma-ray characteristics and the absence of a radio signal (*12*) from the CTA 1 pulsar are suggestive of the family of outer-gap or slot-gap model descriptions for energetic pulsars (*24*–*26*). These outer-magnetosphere models naturally generate gamma-ray emission over a broad range of phase, with superposed sharp peaks resulting from caustics in the pattern of the emitted radiation. Because the emission is predicted to cover such a large area of the sky (>>1 sr) in such models, the total radiated luminosity as inferred from the observed pulsed flux could result in an efficiency as high as 10%, depending on the magnetic inclination angle. The absence of the radio signal is readily explained by misalignment of a narrow radio beam and our line of sight. Both conditions can be met if we see the pulsar at a large angle with respect to the spin and magnetic field axes, but only a detailed model can quantify the viewing geometry of the CTA 1 pulsar. Spectral cut-offs at energies of 1 to 10 GeV that would be indicative of a polar cap mechanism with attenuation of outgoing photons via magnetic pair creation (*27*) or curvature radiation-reaction limited acceleration in an outer gap (*28*) are not yet discernible.

Our detection of a new gamma-ray pulsar during the initial operation of the Fermi LAT implies that there may be many gamma-ray–loud but x-ray– and radio-quiet pulsars.

Although 3EG J0010+7309 was long suspected to be a gamma-ray pulsar because of its clear association with a SNR at ~10° Galactic latitude, it is also fairly typical of many unidentified *EGRET* sources. If the radio remnant CTA 1 was located at low Galactic latitudes, it could have been more difficult to recognize because of the higher and structured radio background of the Galactic disk. About 75% of the low Galactic latitude *EGRET* sources ($|b|$<10°, ~100 objects in the 3EG catalog and CTA 1 just on the edge of this region) are still unidentified, although several are associated with SNRs.

The unidentified low Galactic latitude *EGRET* sources represent the closer and brighter objects of a Galaxy-wide population of gamma-ray sources. *EGRET* was not sensitive enough to discern the more distant sources, which blurred into the diffuse Galactic emission. A model Galactic population conforming to the *EGRET* measurements (*29*), distributed in galacto-centric distance and height above the disk, yields several thousand sources of typical >100-MeV luminosities in the range of 6×10^{34} to 4×10^{35} erg s^{-1}. The CTA 1 pulsar with an isotropic luminosity above 100 MeV of ~6×10^{34} erg s^{-1} falls in the range required for these sources. The CTA 1 pulsar detection implies that gamma-loud but radio- and x-ray–faint pulsars are likely to be detectable in a fair fraction of the remnants of massive star deaths. Topics as diverse as the SN rate in the Galaxy, the development of young (including historical) SNRs, and the physics of pulsar emission can then be studied.

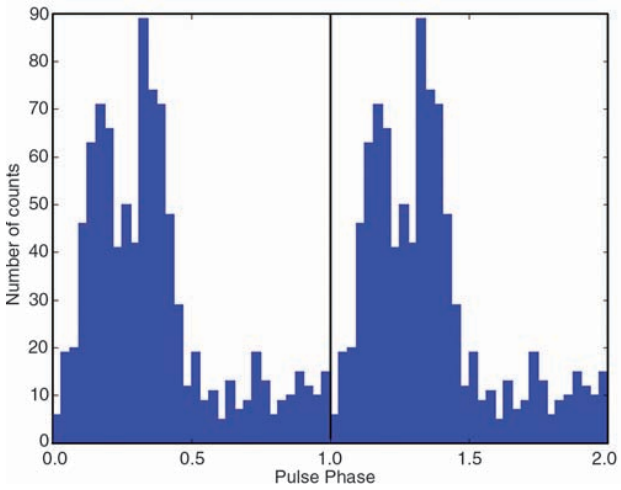

Fig. 3. Gamma-ray (>100 MeV) light-curve of the pulsar in CTA 1 shown over two periods of rotation with a resolution of 32 phase bins per period (corresponding to ~10 ms per bin). The two maxima in the broad emission feature each have a full width at half maximum of ~0.12 and are separated by ~0.2 in phase. Overall, the LAT pulsar light-curve is similar to the gamma-ray light-curve of the *EGRET* pulsar PSR B1706-44 (*23*).

References and Notes

1. D. E. Harris, J. A. Roberts, *Publ. Astron. Soc. Pac.* **72**, 237 (1960).
2. D. E. Harris, *Astrophys. J.* **135**, 661 (1962).
3. J. L. Caswell, *Mon. Not. R. Astron. Soc.* **136**, 11 (1967).
4. W. Sieber, C. G. T. Haslam, C. J. Salter, *Astron. Astrophys.* **74**, 361 (1979).
5. W. Sieber, C. J. Salter, C. J. Mayer, *Astron. Astrophys.* **103**, 393 (1981).
6. S. Pineault *et al.*, *Astron. J.* **105**, 1060 (1993).
7. S. Pineault *et al.*, *Astron. Astrophys.* **324**, 1152 (1997).
8. F. Mavromatakis *et al.*, *Astron. Astrophys.* **353**, 371 (2000).
9. P. Slane *et al.*, *Astrophys. J.* **485**, 221 (1997).
10. P. Slane *et al.*, *Astrophys. J.* **601**, 1045 (2004).
11. F. D. Seward, B. Schmidt, P. Slane, *Astrophys. J.* **453**, 284 (1995).
12. J. P. Halpern *et al.*, *Astrophys. J.* **612**, 398 (2004).
13. R. C. Hartman *et al.*, *Astrophys. J.* **123** (suppl.), 79 (1999).
14. K. T. S. Brazier *et al.*, *Mon. Not. R. Astron. Soc.* **295**, 819 (1998).
15. S. J. Sturner, C. D. Dermer, J. Mattox, *Astron. Astrophys.* **120** (suppl.), 445 (1996).
16. P. F. Michelson *et al.*, *Proceedings of 1st GLAST Symposium*, S. Ritz, P. Michelson, C. Meegan, Eds. (American Institute of Physics, New York, 2007).
17. W. B. Atwood *et al.*, *Astrophys. J.* **652**, L49 (2006).
18. S. M. Ransom, thesis, Harvard University (2001), available at http://www.cv.nrao.edu/~sransom/presto/.
19. G. B. Hobbs, R. T. Edwards, R. N. Manchester, *Not. R. Astron. Soc.* **369**, 655 (2006).
20. D. A. Smith *et al.*, *Astron. Astrophys.*, in press; preprint available at http://adsabs.harvard.edu/abs/2008arXiv0810.1637S.
21. Extrapolation of the present pulsar ephemeris back to the archival epochs results in a large range of uncertainty for the period. Searches in *XMM* data by members of the Fermi LAT collaboration are not yet conclusive.
22. T. Gold, *Nature* **221**, 25 (1969).
23. D. J. Thompson *et al.*, *Astrophys. J.* **465**, 385 (1996).
24. K. Hirotani, preprint available at http://arxiv.org/abs/0809.1283v1 (2008).
25. A. K. Harding, J. V. Stern, J. Dyks, M. Frackowiak, *Astrophys. J.* **680**, 1378 (2008).
26. R. W. Romani, I. A. Yadigaroglu, *Astrophys. J.* **438**, 314 (1995).
27. M. G. Baring, *Adv. Space Res.* **33**, 552 (2004).
28. R. W. Romani, *Astrophys. J.* **470**, 469 (1996).
29. G. Kanbach *et al.*, *Astron. Astrophys.* **120** (suppl.), 461 (1996).
30. G. Hobbs *et al.*, *Mon. Not. R. Astron. Soc.* **360**, 974 (2005).

31. The Fermi LAT Collaboration acknowledges the generous support of a number of agencies and institutes, including NASA and the U.S. Department of Energy in the United States; the Commissariat l'Energie Atomique and the Centre National de la Recherche Scientifique/Institut National de Physique Nuclaire et de Physique des Particules in France; the Agenzia Spaziale Italiana and the Istituto Nazionale di Fisica Nucleare in Italy; the Ministry of Education, Culture, Sports, Science and Technology, the High Energy Accelerator Research Organization, and JAXA in Japan, and the K. A. Wallenberg Foundation and the Swedish National Space Board in Sweden.

Supporting Online Material

www.sciencemag.org/cgi/content/full/1165572/DC1
Fig. S1

5 September 2008; accepted 8 October 2008
Published online 16 October 2008;
10.1126/science.1165572
Include this information when citing this paper.

Observation of Pulsed γ-Rays Above 25 GeV from the Crab Pulsar with MAGIC

The MAGIC Collaboration*

One fundamental question about pulsars concerns the mechanism of their pulsed electromagnetic emission. Measuring the high-end region of a pulsar's spectrum would shed light on this question. By developing a new electronic trigger, we lowered the threshold of the Major Atmospheric γ-ray Imaging Cherenkov (MAGIC) telescope to 25 giga–electron volts. In this configuration, we detected pulsed γ-rays from the Crab pulsar that were greater than 25 giga–electron volts, revealing a relatively high cutoff energy in the phase-averaged spectrum. This indicates that the emission occurs far out in the magnetosphere, hence excluding the polar-cap scenario as a possible explanation of our measurement. The high cutoff energy also challenges the slot-gap scenario.

It is generally accepted that the primary radiation mechanism in pulsar magnetospheres is synchrotron-curvature radiation. This occurs when relativistic electrons are trapped along the magnetic field lines in the extremely strong field of the pulsar. Secondary mechanisms include ordinary synchrotron and inverse Compton scattering. It is not known whether the emission of electromagnetic radiation takes place closer to the neutron star (NS) [the polar-cap scenario (*1*–*3*)] or farther out in the magnetosphere [the slot-gap (*4*–*6*) or outer-gap (*7*–*9*) scenario (Fig. 1)]. The high end of the γ-ray spectrum differs substantially between the near and the far case. Moreover, current models of the slot gap (*6*) and the outer gap (*8*, *9*) differ in their predicted γ-ray spectra, even though both gaps extend over similar regions in the magnetosphere. Therefore, detection of γ-rays above 10 GeV would allow one to discriminate between different pulsar emission models.

At gamma-ray energies (E) of ~1 GeV, some pulsars such as the Crab (PSR B0531+21) are among the brightest γ-ray sources in the sky. The Energetic γ-ray Experiment Telescope (EGRET) detector, aboard the Compton γ-ray Observatory (CGRO), measured the γ-ray spectra of different pulsars only up to $E \approx 5$ GeV because of its small detector area (~0.1 m^2) and the steeply falling γ-ray fluxes at higher energies. At $E > 60$ GeV, Cherenkov telescopes (*10*) are the most sensitive instruments because of their large detection areas of $\geq 10^4$ m^2. But, in spite of several attempts, no pulsar has yet been detected at such energies (*11*–*16*). This suggests a spectral cutoff; that is, that the pulsar's emission drops off sharply, between a few giga–electron volts and a few tens of giga–electron volts.

The Crab pulsar is one of the best candidates for studying such a cutoff. Its spectrum has been measured by EGRET (*17*) up to $E \approx 5$ GeV without a clear cutoff being seen. Earlier observations with the 17-m-diameter Major Atmospheric γ-ray Imaging Cherenkov (MAGIC) (*18*) telescope (Canary Island of La Palma, 2200 m above sea level) revealed a hint of pulsed emission at the 2.9 standard deviation (σ) level above 60 GeV (*19*, *20*). To verify this result, we developed and installed a new trigger system that lowered the threshold of MAGIC from ~50 GeV to 25 GeV [supporting online material (SOM) text] (*21*).

We observed the Crab pulsar between October 2007 and February 2008, obtained 22.3 hours of good-quality data, and detected pulsed emission above 25 GeV. The pulsed signal (Fig. 2) has an

*The full list of authors and affiliations is presented at the end of this paper.